Springer

Journal of Mechanical Science and Technology 22 (2008) 1821~1829

Journal of Mechanical Science and Technology

www.springerlink.com/content/1738-494x
DOI 10.1007/s12206-008-0614-3

Investigation on hydrodynamics and mass transfer characteristics of a gas-liquid ejector using three-dimensional CFD modeling

Tony Utomo[1], Zhenhua Jin[1], MSq Rahman[1], Hyomin Jeong[2] and Hanshik Chung[2,*]

[1]*Graduate School of Department of Mechanical and Precision Engineering, Gyeongsang National University, 445 Inpyeong-Dong, Tongyeong, Gyeongsangnamdo 650-160, Korea*

[2]*Department of Mechanical and Precision Engineering, Gyeongsang National University, 445 Inpyeong-Dong, Tongyeong, Gyeongsangnamdo 650-160, Korea*

(Manuscript Received August 21, 2007; Revised June 9, 2008; Accepted June 18, 2008)

Abstract

An investigation of the gas-liquid ejector has been carried out to study the influence of operating conditions and ejector geometries on the hydrodynamics and mass transfer characteristics of the ejector by using three-dimensional CFD modeling. The CFD results were validated with experimental data. Flow field analysis and prediction of ejector performance were also conducted. Variations of the operating conditions were made by changing the gas-liquid flow rates ratio in the range of 0.2 to 1.2. The length to diameter ratio of mixing tube (L_M/D_M) was also varied from 4 to 10. CFD studies show that at L_M/D_M=5.5, the volumetric mass transfer coefficient increases with respect to gas flow rate. Meanwhile, at L_M/D_M=4, the plot of volumetric mass transfer coefficient to gas-liquid flow rate ratio reaches the maximum at gas-liquid flow rate ratio of 0.6. This study also shows that volumetric mass transfer coefficient decreases with the increase of mixing tube length.

Keywords: Hydrodynamics; Mass transfer; Ejector; CFD; Gas-liquid

1. Introduction

In the field of chemical and biochemical reaction engineering, there has been increasing interest in jet loop reactors during the last decade because of their high efficiency in gas dispersion resulting in high mass transfer rate. Jet loop reactors are also used in hydrogenation and chlorination in the chemical process industry. Many other examples concerning the use of jet loop reactor can also be found, e.g., in the papers of Daucher [1], Zahradnik and Rylek [2], Cramers et al. [3,4], Gracia Salas and Cotera-Flores [5], Kim and Choi [6], and Jeong et al. [7].

The principle of this reactor type is the utilization of the kinetic energy of a high velocity liquid jet to entrain the gas phase and to create a fine dispersion of the two phases. Mixing and process equipment are the essential units of any chemical industry that utilize this type of reactor. Due to their favorable mass transfer and mixing characteristics, ejectors are being increasingly used as gas-liquid contactor in these processes. A standard ejector, shown schematically in Fig. 1, consists of a nozzle, suction chamber, mixing tube, diffuser and draft tube. The primary fluid, typically liquid, is pumped into the system at high velocity through a nozzle. According to Bernoulli's principle, a low-pressure region is created in the suction chamber, into which the secondary fluid gets drawn. Typically this secondary fluid is in the gas phase. The gas and liquid phases are mixed and a gas-liquid dispersion is created in the mixing tube. The pressure is recovered in the diffuser at the exit of the mixing tube. When the secondary fluid is sucked into the suction chamber, the gas and liquid flows are initially coaxial, consisting of an annular secondary fluid flow and a primary fluid jet. This jet flow persists for a certain

*Corresponding author. Tel.: +82 55 640 3184, Fax.: +82 55 640 3188
E-mail address: hschung@nongae.gsnu.ac.kr

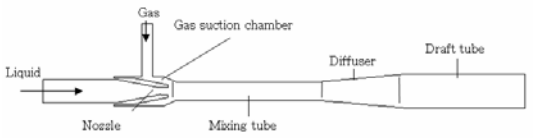

Fig. 1. Schematic diagram of ejector.

distance in the mixing tube. According to Witte [8], a so-called mixing shock occurs at a particular location in the mixing tube. The two phase flow changes into a homogeneous bubble flow from jet flow in the region of mixing shock. This flow-pattern transition is accompanied by a sudden pressure build-up. A part of the kinetic energy of the flow is dissipated in the shock and gas-liquid dispersion develops. Downstream of this mixing zone, both phases flow homogeneously through the remaining part of the ejector. When the gas-liquid flow stream leaves the ejector, a secondary dispersion of bubbles is created in the bulk fluid of the reactor vessel. The dispersion finally disengages into two separate fluid phases in the vessel tank. According to Cunningham and Dopkin [9], the location of the mixing shock zone is an important key of the ejector performance. The optimum dispersion efficiency is achieved when the liquid jet breaks up just at the end of the mixing tube. If the jet disintegration occurs earlier, the flow of the homogeneous gas-liquid mixture through the remaining part of the mixing tube will result in excessive friction losses. On the other hand, if the mixing tube is too short, the jet does not break up and accordingly, the momentum transport between the phases does not occur. As a result, the ejector efficiency decreases abruptly. Obviously, the occurrence of the jet break-up and the position of the mixing shock zone in the mixing tube depend on the gas and liquid flow rate, and the ejector parameters such as the length of mixing tube.

The effect of different operating conditions and ejector geometry parameters on the performance of ejector has been experimentally investigated by several researchers [10-15]. From those authors, Dirix and van de Wiele [13] and Cramers et al. [15] have studied in more detail concerning the influence of geometrical parameter of ejector such as mixing tube length on the hydrodynamics and mass transfer characteristics of ejector. Unfortunately, there were contradictory results in their experiments, especially on the influence of the mixing tube on the volumetric mass transfer coefficient. According to the experiments of Dirix and van de Wiele [13], the mixing tube length had no influence on the volumetric mass transfer coefficient. On the other hand, Cramers et al. [15] found the opposite fact that the volumetric mass transfer coefficient was influenced by the mixing tube length. However, they demonstrated that the mass transfers of both the ejector and vessel were influenced by the flow regime in the ejector. Therefore, there is a need to develop a better understanding of hydrodynamics of the ejector systems.

Recently, with the rapid development of numerical solution methods, some researchers have attempted to apply computational fluid dynamics (CFD) in modeling the flow inside ejectors. Riffat and Omer [16] used a commercial CFD package to predict the performance of a methanol-driven ejector. Unfortunately, the results were not validated through any experimental data. Choi et al. [17] investigated numerically the flow of subsonic/sonic ejector of a bleed pump. Rusly et al. [18] simulated the flow through ejector used in cooling system. Sriveerakul et al. [19] investigated the performance of steam ejector used in a refrigeration system. Although there are numbers of papers that have investigated the ejector numerically using CFD, most of them did two-dimensional modeling. In this case, the CFD analysis could not account for the effect of three-dimensional flow phenomena in the suction chamber and in a part of the mixing tube where the mixing phenomena occur.

In this study, a CFD package (STAR CD) is employed to analyze a small water ejector which is equipped in an experimental mixing loop reactor. The ejector is modeled in three-dimensional geometry in order to get better agreement between simulation results and the real conditions. The effect of operating conditions and geometries on its hydrodynamics and mass transfer characteristics are investigated and validated with actual values obtained from experiment.

2. Experimental description

A schematic diagram of a mixing loop reactor system with ejector is presented in Fig. 2. The mixing loop reactor consists of ejector, vessel tank, make-up water tank and centrifugal pump. The inlet pressure is measured at point 1. Suction pressure and outlet pressure are collected from the entrance of the secondary fluid (2) and outlet of the vessel tank, respectively.

In the present study, the configuration of ejector has a mixing tube diameter (D) of 22 mm and diffuser outlet diameter of 40 mm (i.e., diffuser angle of 3.5)

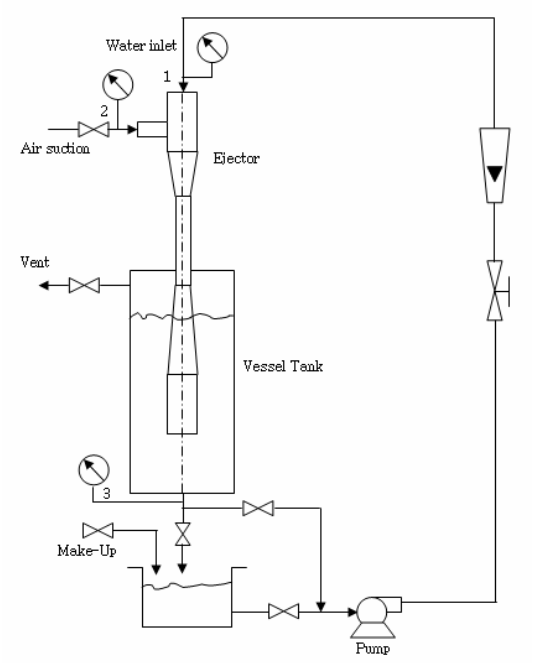

Fig. 2. Schematic diagram of mixing loop reactor.

and a draft tube length (L) of 100 mm. The mixing tube lengths are varied between 88 and 220 mm with the nozzle diameter of 8.5 mm.

3. CFD modeling

In this research, five different models of ejector were developed to investigate the influence of mixing tube length on the mass transfer characteristics. These models have variation in length of the mixing tube of 88, 120, 150, 176 and 220 mm. The ejector geometry is modeled on a commercial CAD software package, CATIA. STAR CD software is employed for generating grid and CFD solver.

3.1 Geometries and grids

As proposed, Pro-Star Auto mesh of STAR CD software package was used to create the calculation domain and grid elements of the model. The mesh and model were created in a three-dimensional (3D) domain to account for the local details of the complex flow structure taking place during ejector operation. The geometries of the calculation domain of the modeled gas-liquid ejectors are described in Fig. 3. For preliminary results, the grid was initially made of about 100,000 structured trimmed quadrilateral cells

Fig. 3. The ejector model with trim cell mesh generation (inset: real ejector).

with variation of sub layer thickness to accommodate the curving nature and sharp angle of the ejector geometries. The concentration of grid density is focused on the areas where significant phenomena are expected. In order to obtain the grid independent result, reasonable numbers of iterations were conducted by refining the mesh in every stage of simulation. After several simulations, the fixed number of cells with grid-independent result was obtained as 395,240 cells. In this study, the grid cell volume used in the CFD simulation of ejector was set for about 400,000 cells.

3.2 Case setup

As the working fluids used in this research are water as primary fluid and air as secondary fluid, so the assumption of incompressible flow is appropriate. Hence, the *standard k-*ε with high Reynolds number is selected to govern the turbulence characteristics. The near wall treatment was left as the *standard wall function*, which gives reasonably accurate results for the wall bounded with very high Reynolds number flow. The thermophysical properties of the working fluids were obtained at 293 K and 300 K, respectively, for water and air. The turbulence intensity was set to be 3.5% for primary fluid.

3.3 Boundary conditions

Boundary conditions of two faces entering a primary nozzle and ejector were set as velocity inlet and pressure inlet, respectively. The face at the exit of ejector was set as outlet boundary. At the inlet boundary, the velocity components, turbulent kinetic energy and turbulent dissipation rate have to be specified. The applied velocity at the inlet boundary was based on the experimentally measured volumetric flow rate, which was 4 m^3/h of water. The velocity of air was based on the Q_G /Q_L ratio in the range of 0.2 to 1.2. This ratio was selected in order to maintain bubbly flow regimes inside the ejector [13].

3.4 Calculation of volumetric mass transfer coefficient

Based on their experimental results, Dirix and van de Wiele [13] recommend empirical correlations for mass transfer coefficient on the liquid side for a down flow ejector as

$$k_L a = 5.4\times10^{-3}(\in)^{0.66}\varepsilon_G\left(\frac{d_N}{d_D}\right)^{0.66} \quad (1)$$

$$k_L a = 8.5\times10^{-4}(\in)^{0.66}\left(\frac{d_N}{d_B}\right)^{0.66} \quad (2)$$

where $$\varepsilon_G = \frac{Q_G}{Q_G + Q_L} \quad (3)$$

Eq. (1) is used to calculate the volumetric mass transfer coefficient of the ejector in the bubbly flow regimes. Meanwhile, Eq. (2) is used for the jet flow regimes inside the ejector. In this research, Eq. (1), (2), and (3) will be used for the analysis of hydrodynamics and mass transfer characteristics in the ejector.

4. Results and discussion

4.1 Validation

Fig. 4 shows the effect of liquid flow rate on inlet pressure, outlet pressure and suction pressure of the ejector. In the case of inlet pressure, there is an increase of inlet pressure with respect to the increase of liquid flow rate. The circle dot mark represents the experimental data while the solid line is for CFD simulation. It can be seen that there is a good agreement between experiment and CFD. In the case of outlet pressure, though, there is a small discrepancy between experiment and CFD. This discrepancy is caused mostly by the location of pressure measurement at the outlet of the ejector. Unlike the data from experiment which was taken at the outflow pipe of vessel tank, the CFD outlet pressure data was taken at the end of ejector draft tube. Those circumstances result in the different pressure drop at the location where the outlet pressure data were taken between CFD and experiment. However, both of those data show the same trend. In the case of suction pressure, both data from experiment and CFD show that it is nearly independent with respect to liquid flow rate. It also can be seen that there is a good agreement between CFD and experiment data. Thus, the hydrodynamics

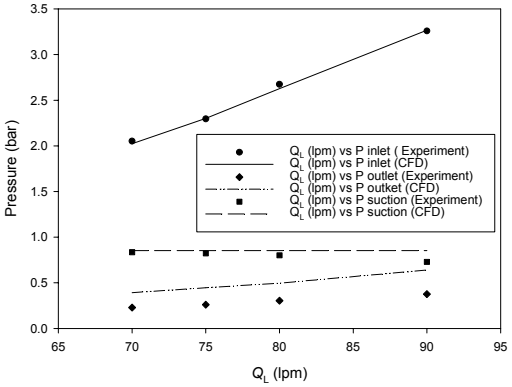

Fig. 4. The influence of liquid flow rate on inlet pressure, outlet pressure and suction pressure of ejector.

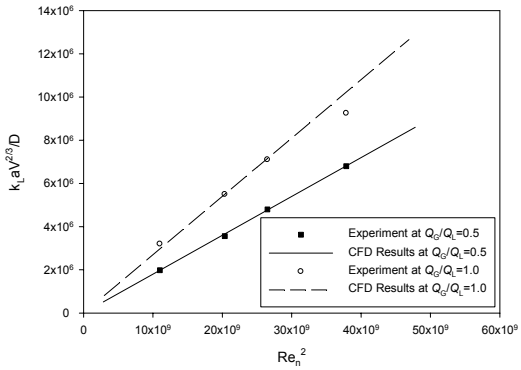

Fig. 5. Influence of Reynolds number on mass transfer in the ejector.

parameter of CFD data is valid with respect to experiment data.

Fig. 5 shows the influence of Reynolds number at nozzle on the mass transfer number in the ejector. This graph is used to validate the CFD data in the manner of mass transfer characteristic. The experimental data is obtained from Dirix and Van de Wiele [13]. From this graph, it can be seen that for a constant ratio of Q_G/Q_L the mass transfer number is found to be proportional to Re_n^2, which represents the hydrodynamics characteristic of the ejector. The results obtained from CFD have a good agreement with that of experiment. All of those validation data of hydrodynamics and mass transfer indicate that the codes of simulation in these CFD studies are valid. Hence, for further CFD studies, the codes were kept constant for all other simulations. Thus, henceforth, there is no other empirical/fitting parameter and all results are truly predictive.

4.2 Hydrodynamics and mass transfer characteristics along the ejector

Fig. 6 shows the predicted pressure distribution at the centerline of the ejector from the tip of nozzle to the outlet of draft tube for various Q_G/Q_L. This graph indicates the gas-liquid flow rate ratio is influencing the jet break-up and the position of the mixing shock zone in the mixing tube. The mixing zone location is shifted from the mixing tube entrance at lower Q_G/Q_L towards the ejector outlet at higher Q_G/Q_L.

Fig. 7 shows the prediction of distribution of energy dissipation rate for various Q_G/Q_L along the ejector from the nozzle tip until the end of the mixing tube. It can be seen that the maximum energy dissipation rate is achieved at Q_G/Q_L=0.2. The average of the dissipation rate along the mixing tube decreases contrary to the increase of Q_G/Q_L. The interesting phenomenon is the location where the maximum energy dissipation rate occurs is shifted towards the exit of mixing tube with respect to gas-liquid flow rate ratio. According to Witte [8], this phenomenon is related to the location of mixing shock where the jet break-up occurs. In this phenomenon, the jet breaks up when a part of kinetic energy of the flow is dissipated in the shock creating the gas-liquid dispersion. By increasing the gas flow rate, the coaxial annular gas flow around the core of the primary fluid jet is elongated in the mixing tube, causing the shifted location of mixing shock area. This phenomenon is clearly illustrated in Fig. 8.

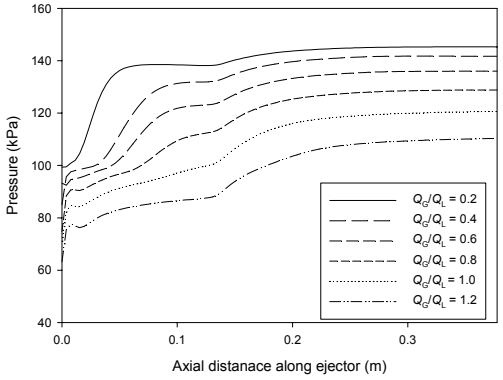

Fig. 6. Pressure distribution along the ejector for various Q_G/Q_L.

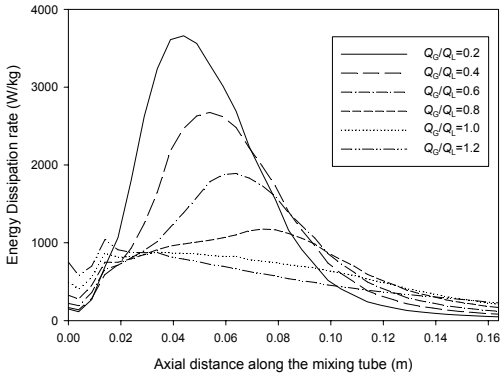

Fig. 7. Distribution of energy dissipation rate inside mixing tube for various Q_G/Q_L.

Fig. 8 shows the contours of air fraction as a secondary fluid in the water at various axial locations for Q_G/Q_L equal to 0.2, 0.6 and 1.2. The axial locations are at 3.9, 13.9, 43.9, 73.9 and 120 mm downstream of the nozzle tip. The reasons for selecting those locations are as follows: at 3.9 mm downstream of the nozzle tip - to account for the mixing phenomena that are predicted to occur in this area; at 13.9 mm and 120 mm downstream of nozzle tip for the entrance and the end of mixing tube, respectively. The other three locations (13.9, 43.9 and 73.9 mm) are picked to compare the visualization of mixing phenomena for three different Q_G/Q_L ratios inside the mixing tube. From this figure, it is seen that at 3.9 mm downstream of the nozzle tip, the mixing phenomenon occurs at Q_G/Q_L=0.2, while this phenomenon exists neither at Q_G/Q_L=0.6 nor at Q_G/Q_L=1.2. At the entrance of mixing tube, the dispersion of gas phase into liquid phase is almost complete at Q_G/Q_L=0.2, while the gas phase builds the coaxial annular gas flow around the core of primary fluid jet at Q_G/Q_L=0.6 and Q_G/Q_L=1.2. However, the dispersion of a small part of gas takes place at the top side of the mixing tube. At 43.9 mm downstream of the nozzle tip, the flow becomes almost homogeneous at Q_G/Q_L=0.2, while at Q_G/Q_L=0.6 the mixing is still ongoing; meanwhile the gas phase is still occupying 1/3rd of the cross sectional area of the tube at the bottom side of this illustration. When the cross sectional area is shifted downstream at 73.9 mm from the nozzle tip or in the middle of the mixing tube, the two phases are completely mixed and become homogeneous flow at Q_G/Q_L=0.2. Meanwhile, at Q_G/Q_L=0.6, the mixing phenomenon is almost complete; at Q_G/Q_L=1.2, the gas stream at the bottom of the mixing tube decreases to smaller part and the mixing is still growing continuously. Finally, at the exit of the mixing tube, the flow becomes completely homogeneous for Q_G/Q_L=0.2 as mentioned previously and also for Q_G/Q_L=0.6. In contrast with those results,

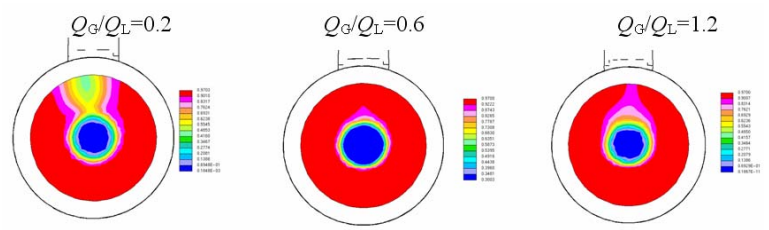

(a) 3.9 mm from the nozzle tip

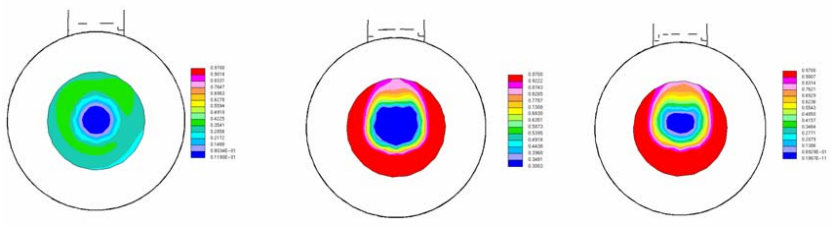

(b) 13.9 mm from the nozzle tip

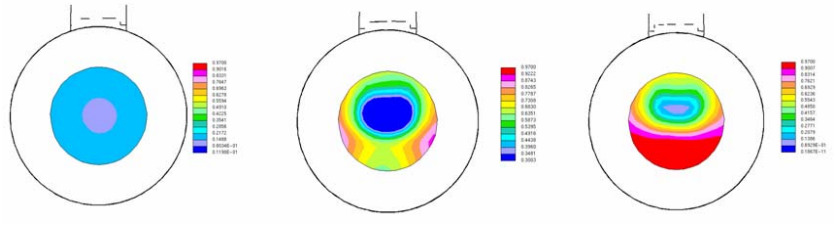

(c) 43.9 mm from the nozzle tip

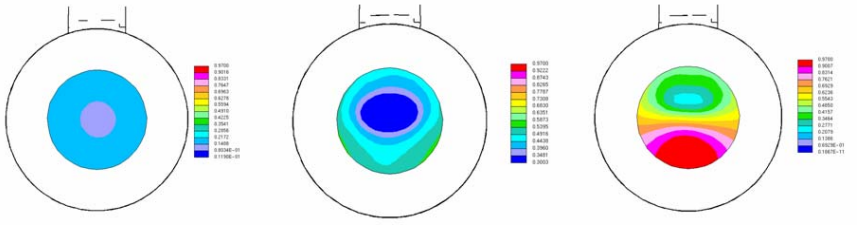

(d) 73.9 mm from the nozzle tip

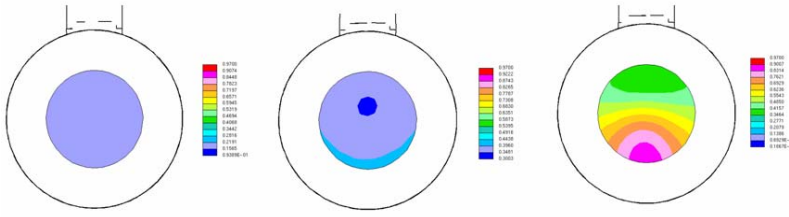

(e) 120 mm from the nozzle tip

Fig. 8. Mixing phenomena in cross sectional view inside the mixing tube.

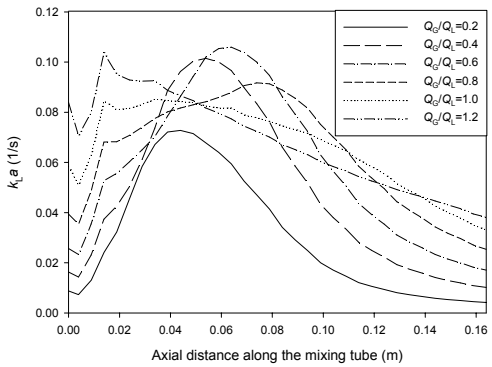

Fig. 9. Distribution of volumetric mass transfer coefficient for various Q_G/Q_L along the mixing tube.

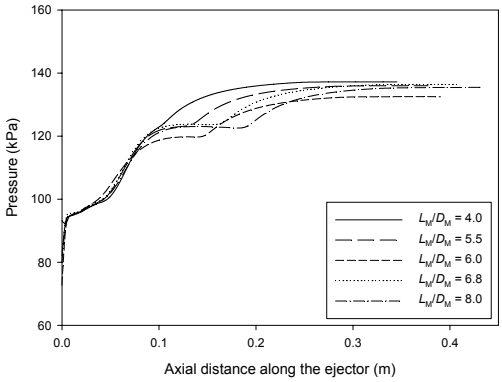

Fig. 10. Pressure distribution, at the centerline, along the ejector for various L_M/D_M.

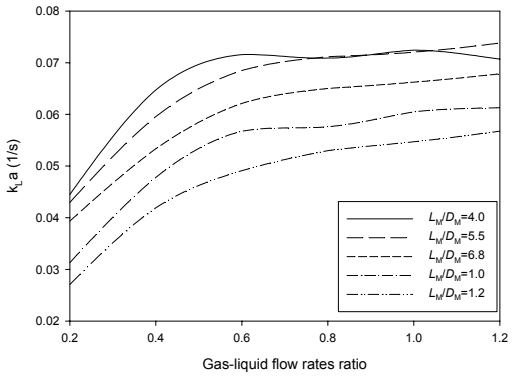

Fig. 11. Influence of mixing tube length on the volumetric mass transfer coefficient.

the mixing is still developing at Q_G/Q_L=1.2 and homogeneous flow is not obtained then. Thus, if the gas flow is increased to higher values, the jet break-up could not occur in the mixing tube, but it may occur in the diffuser or in the draft tube. When the jet break-up takes place in the diffuser or draft tube, the mass transfer coefficient will decrease.

Fig. 9 shows the distribution of volumetric mass transfer coefficient for various Q_G/Q_L along the mixing tube from the nozzle tip. The volumetric mass transfer coefficient is inversely related to the energy dissipation rate distribution (Fig. 7 and Fig. 9). It can be seen in Fig. 7, where the energy dissipation rate distribution at Q_G/Q_L=0.2 shows the highest value among the other gas-liquid flow rate values, but it has the lowest value of volumetric mass transfer coefficient. This phenomenon is caused by the fact that the volumetric mass transfer coefficient depends not only on the energy dissipation rate, but also on the gas fraction.

4.3 The influence of mixing tube length

Fig. 10 shows the predicted pressure distribution, at the centerline of the ejector from the nozzle tip to the exit of ejector for five different L_M/D_M ratios: 4, 5.5, 6.8, 8 and 10 at Q_G/Q_L=0.6. The pressure at the nozzle tip for any L_M/D_M ratio is the same. The sudden pressure build-up is also started almost at the same location. Accordingly, the place where the mixing shock started is located at the same location, independent of the mixing tube length. However, the mixing shock is ended in a different location. Therefore, the mixing shock volume depends on the mixing tube length and the dispersion of gas into liquid occurs inside it. Hence, the mass transfer coefficient varies as well.

Fig. 11 clearly illustrates that an ejector with longer mixing tube creates lower volumetric mass transfer coefficient compared to one with shorter mixing tube. It is seen that by increasing L_M/D_M ratio, the volumetric mass transfer coefficient decreases in any gas-liquid flow rate ratios. It is obvious when the mixing tube length is increased then the pressure drop is also increased. Thus, a part of the energy supplied by the high velocity jet is used to overcome this pressure drop instead of gas dispersion. Hence, the supplied energy is not effectively used for mixing both phases. As a result, the k_La value becomes low. However, for an ejector with L_M/D_M=4, at a gas-liquid flow rate ratio from 0.2 to 0.6 the volumetric mass transfer coefficient is higher than that of any other L_M/D_M ratios. By increasing the Q_G/Q_L ratio more than 0.6, the k_La value then decreases. This phenomenon can occur in an ejector with shorter mixing tube, because the increase of gas flow rate causes the jet flow to occur longer in the mixing tube. Then, the mixing

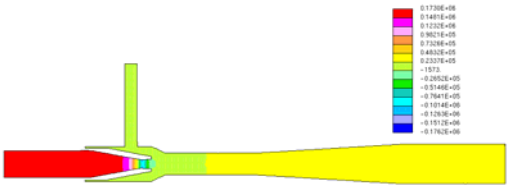

(a) Q_G/Q_L=0.2

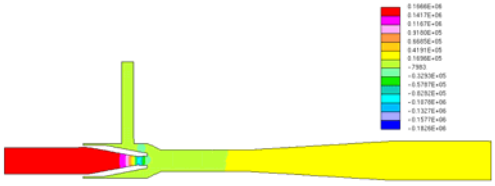

(b) Q_G/Q_L=0.6

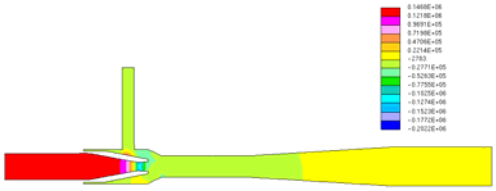

(c) Q_G/Q_L=1.2

Fig. 12. Contour of pressure along the ejector with L_M/D_M of 4 at various Q_G/Q_L.

shock is shifted towards the exit of the ejector. In this case, the mixing shock occurs at the diffuser. This condition causes ineffective mixing phenomena of both phases. Fig. 12 shows the predicted pressure contour along the ejector with L_M/D_M=4 at Q_G/Q_L of 0.2, 0.6 and 1.2. It illustrates the shifting of mixing shock with respect to the increasing of gas flow rate.

5. Conclusions

A CFD model is developed to elucidate the hydrodynamics characteristics of an ejector. The model was first validated by varying the primary fluid flow rate, and then the inlet pressure, suction pressure and outlet pressure were calculated. The CFD results have a good agreement with experimental data. The second validation was made by comparing the CFD results to the experimental results of Dirix and Van de Wiele [13] to account the effect of hydrodynamics of ejector on the mass transfer characteristics. The CFD result also matches the experimental data very well. By this validated code of simulation, predictions were made for different geometries of mixing tube length.

From this study, it can be concluded that the gas-liquid flow rate ratio has a significant effect on the hydrodynamics and mass transfer characteristics of an ejector. In this research, the volumetric mass transfer coefficient increases with respect to the gas flow rate of the ejector with a minimum length of mixing tube of 120 mm (L_M/D_M=5.5). For an ejector with mixing tube length of 88 mm (L_M/D_M=4), the volumetric mass transfer coefficient reaches the maximum at a gas-liquid flow rate ratio of 0.6. Further increase of gas-liquid flow rate ratio results in a reduction of the volumetric mass transfer coefficient. It also can be concluded that the mixing tube length influences the volumetric mass transfer coefficient of an ejector. This coefficient decreases with the increase of mixing tube length.

Overall, the CFD method is an efficient tool for predicting the hydrodynamics and mass transfer characteristics of an ejector. It can give a good result as a complement to the experimental approach.

Acknowledgement

This research was supported under the project (No.70002054) of ITEP in the Ministry of Knowledge Economy and the second-phase of Brain Korea 21 Project. The authors gratefully acknowledge the support from DAEWON heat plate Co., Ltd.

Nomenclature

d_B : Maximum stable bubble diameter (m)
d_D : Diffuser diameter (m)
d_M : Mixing tube diameter (m)
d_N : Nozzle diameter (m)
k_La : Volumetric mass transfer coefficient (l/s)
Q_G : Volumetric gas flow rate (lpm)
Q_L : Volumetric liquid flow rate (lpm)

Greek letters

ε_G : Gas fraction
$\in$: Energy dissipation rate (W/kg)

References

[1] H. H. Daucher, Oxygen transfer and circulation rate in activated sludge channels aerated by jets, *Ger. Chem. Engng*, 5 (1982) 255-261.
[2] J. Zahradnik and M. Rylek, Design and scale-up of Venturi-tube gas distributors for bubble column reactors, *Collect. Czech. Chem. Commun.,* 56 (1991) 619-635.

[3] P. H. M. R. Cramers, A. A. C. M. Beeneckers and L. L. van Direndonck, Hydrodynamics and Mass Transfer Characteristics of Loop-Venturi Reactor with a Downflow liquid Jet Ejector, *Chem. Engng Sci.,* 47 (1992) 3557-3564.

[4] P. H. M. R. Cramers, L. L. van Direndonck and A. A. C. M. Beeneckers, Influence of the gas density on the gas entrainment rate and gas hold-up in loop-venture reactors, *Chem. Engng Sci.,* 47 (1992) 2251-2256.

[5] S. Gracia Salas and L. B. Cotera Flores, Influence of operating variables on liquid circulation in a 10.5 m^3 jet loop bioreactor, *Biotechnol. Bioengng*, 46 (1995) 408.

[6] H. D. Kim and B. G. Choi, An experimental study of sonic/supersonic ejector flow, *Trans. of KSME*, 26 (5) (2002) 640-647.

[7] H. M. Jeong, H. S. Chung, K. Y. Bae, S. H. Kim and Y. S. Shin, Water cooling characteristics in an enclosed vacuum tank by water driven ejector, *Journal of Mechanical Science and Technology*, 19 (1) (2005) 164-172.

[8] J. H. Witte, Mixing shocks in two phase flow, *J. Fluid Mech.,* 36 (1996) 639-655.

[9] R. G. Cunningham and R. J. Dopkin, Jet Breakup and Mixing Throat Lengths for the Liquid Jet Gas Pump, *Trans. ASME – J. Fluids Engng,* 96 (1974) 216-226.

[10] P. A. Bhat, A. K. Mitra and A. N. Roy, Momentum transfer in a horizontal liquid jet ejector, *Canadian Journal of Chemical Engineering*, 50 (1972) 313-317.

[11] M. N. Biswas and A. K. Mitra, Momentum transfer in horizontal multi-jet liquid-gas ejector, *Canadian Journal of Chemical Engineering*, 59 (1981) 634-637.

[12] S. R. Bhutada and V. G. Pangarkar, Gas induction and hold-up characteristics of liquid jet loop reactors, *Chemical Engineering Communication*, 61 (1987) 239-261.

[13] C. A. M. C. Dirix and K. van der Wiele, Mass Transfer in Jet Loop Reactor, *Chem. Engng Sci.*, 45 (1990) 2333-2340.

[14] P. Havelka, V. Linek, J. Sinkule, J. Zahradnik and M. Fialova, Effect of the ejector configuration on the gas suction rate and gas hold-up in ejector loop reactors, *Chem. Engng Sci.*, 52 (1997) 1701-1713.

[15] P. H. M. R. Cramers and A. A. C. M. Beeneckers, Influence of the ejector configuration, scale and the gas density on the mass transfer characteristics of gas-liquid ejectors, *Chem. Engng Sci.,* 82 (2001) 131-141.

[16] S. B. Riffat, and S. A. Omer, CFD modeling and experimental investigation of an ejector refrigeration system using methanol as the working fluid, *International Journal of Energy Reservation*, 25 (2001) 115~128.

[17] B. G. Choi, B. S. Koo, H. D. Kim and D. J. Kim, Computations of Bleed Pump Type Subsonic/Sonic Ejector Flow, *Trans. of KSME*, 25 (12) (2001) 269-276.

[18] E. Rusly, A. Lu, W. W. S. Charters, A. Ooi and K. Pianthong, CFD analysis of ejector in a combined ejector cooling system, *International Journal of Refrigeration*, 28 (2005) 1092-1101.

[19] T. Sriveerakul, S. Aphornratana and K. Chunnanond, Performance prediction of steam ejector using computational fluid dynamics: Part 1. Validation of the CFD results, *International Journal of Thermal Sciences, The SCI.* 2553, Article in press (2006).